Nonlinear Peltier effect in semiconductors

Mona Zebarjadi[a)]
Department of Electrical Engineering, University of California, Santa Cruz, California 95064, USA

Keivan Esfarjani
Department of Physics, University of California, Santa Cruz, California 95064, USA

Ali Shakouri
Department of Electrical Engineering, University of California, Santa Cruz, California 95064, USA

(Received 12 July 2007; accepted 27 August 2007; published online 18 September 2007)

Nonlinear Peltier coefficient of a doped InGaAs semiconductor is calculated numerically using the Monte Carlo technique. The Peltier coefficient is also obtained analytically for single parabolic band semiconductors assuming a shifted Fermi-Dirac electronic distribution under an applied bias. Analytical results are in agreement with numerical simulations. Key material parameters affecting the nonlinear behavior are doping concentration, effective mass, and electron-phonon coupling. Current density thresholds at which nonlinear behavior is observable are extracted from numerical data. It is shown that the nonlinear Peltier effect can be used to enhance cooling of thin film microrefrigerator devices especially at low temperatures. © *2007 American Institute of Physics*. [DOI: 10.1063/1.2785154]

The Peltier coefficient plays an important role on how good a material is for thermoelectric solid-state refrigeration or power generation. In the linear regime, the Peltier coefficient is independent of the current and it is equal to the product of the Seebeck coefficient by the absolute temperature. If we keep increasing the applied fields to high values, linear relations will no longer be valid. Nonlinear current-voltage characteristics are very common in most active electronic devices. On the other hand, nonlinear thermoelectric effects have not been investigated in detail.

Kulik[1] calculated the electric field dependence of the third-order Peltier coefficient in metals at low temperatures supposing constant inelastic and elastic relaxation times. He showed that this term is proportional to the product of the total relaxation time by the inelastic relaxation time and that it is inversely proportional to the electron effective mass. Grigorenko *et al.*[2] calculated the nonlinear Seebeck coefficient in metals by expanding the distribution function in series of temperature gradients. They found that higher-order nonlinear thermoelectric terms are proportional to the square of the scattering time at the Fermi level. A dimensionless parameter $\omega = l_0 \nabla T/T$ was defined (l_0 is the electron mean free path and T is the temperature) to describe the deviation from local equilibrium and the nonlinearity of the system. Later they extend their theory to the case of two-dimensional metals.[3] Freericks and Zlatic generalized the many-body formalism of the Peltier effect to the nonlinear regime.[4] Nonlinearity of the thermoelectric effects in lower dimensions, such as nanowires[5] and point contacts,[6] has also been investigated using the Landauer formalism. Experimentally, nonlinearity of the Seebeck coefficient has been observed in a one-dimensional ballistic constriction at low temperatures[7] (550 mK) and recently in the measurement of the Seebeck coefficient of single molecule junctions.[8]

On the theoretical side, there has not been any formalism beyond the constant relaxation time approximation to describe the nonlinearity of thermoelectric effects in doped bulk semiconductors. Doped semiconductors are the best candidates for thermoelectric applications so it is important to understand their behavior at experimentally achievable high current densities. At scales larger than the electron de Broglie wavelength, the Boltzmann transport equation (BTE) is the governing equation. The Monte Carlo (MC) technique is considered as one of the most accurate tools to solve BTE. We have developed a Monte Carlo program[9] to simulate thermoelectric transport in GaAs family of materials. The code is three dimensional both in k and r spaces with nonparabolic multivalley band structure. The scattering mechanisms included are ionized and neutral impurities, intravalley polar optical phonons, acoustic phonons, and inter-intravalley nonpolar optical phonons. Pauli exclusion principle is enforced after each scattering process supposing a shifted Fermi sphere as the local electronic distribution. For each valley, the electronic temperature is defined locally as follows:

$$f_v(\mathbf{k}, \mu_v, T_e^v) = \left\{ \exp\left(\frac{E_v[|\mathbf{k} - \mathbf{k}_d^v(\mathbf{r})|] - \mu_v(\mathbf{r})}{k_B T_e^v(\mathbf{r})} \right) + 1 \right\}^{-1},$$

$$T_e^v(\mathbf{r}) = \frac{2}{3k_B} \{ \langle E_v[\mathbf{k} - \mathbf{k}_d^v(\mathbf{r})] \rangle - \langle E_v(\mathbf{r}) \rangle_0 \} + T. \quad (1)$$

Here $\langle E_v(\mathbf{r}) \rangle_0$ is the local average energy of electrons in equilibrium at zero electric field.$\mathbf{k}_d^v(\mathbf{r})$ is the local drift wave vector, which is the average wave vector of all the particles at position $\mathbf{r}$ and in valley v, and μ is the quasiFermi level. Details of adding Pauli exclusion principle in highly doped semiconductors is described in another publication[10] where we showed that using the above definition for electronic temperature results in the correct electronic distribution. The formalism works up to high fields, in the regime where nonparabolic multivalley band structure is valid.

A uniform lattice temperature is enforced along the sample. The sample is subjected to a voltage difference. The resulting potential distribution and current flow are obtained via the Monte Carlo code coupled with a one-dimensional Poisson solver. Dirichlet boundary conditions are used for

[a)]Electronic mail: mona@soe.ucsc.edu

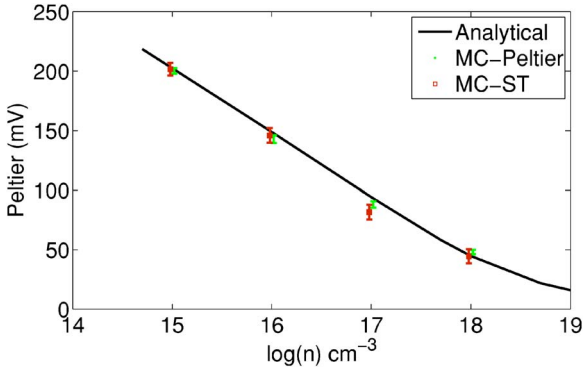

FIG. 1. (Color online) Comparison of Peltier (dots with errorbar) and Seebeck (multiply by the absolute temperature, squares) coefficients obtained from the MC simulation and the analytical results. Figure confirms that the Onsager relation is satisfied. Results are reported for $In_{0.53}Ga_{0.47}As$ at room temperature.

Poisson solver and periodic boundary conditions are supposed in all directions for MC simulation. The Peltier coefficient is defined as $J_Q = \Pi J_e|_{\nabla T=0}$. In the linear transport regime, the Peltier coefficient can be calculated analytically (see for example, Ref. 9). A simple test of the program is to check the agreement between MC data and analytical results. This is confirmed in Fig. 1. The same band structure and relaxation times are used in both cases. In another MC program, we enforce a linear temperature drop along the same bulk sample and we calculate the electrochemical difference of the hot and cold side under open voltage conditions. The Seebeck coefficient is defined as $\nabla\bar{\mu} = eS\nabla T|_{J=0}$, where $\bar{\mu} = \mu + eV$. In Fig. 1 we have also reported the result of the Seebeck coefficient obtained from the later program. This confirms the satisfaction of the Onsager relation and therefore the consistency of simulations.

Supposing a shifted Fermi-Dirac distribution for electrons, the Peltier coefficient is obtainable analytically. After a second order Taylor expansion of the distribution function about k_d (drift wavevector), one finds:

$$\Pi = \frac{-\mu}{e} + \frac{nv_d\varepsilon_d + \frac{5}{3}nv_d\frac{\hbar^2 q_e^2}{2m_d} + \varepsilon_d \mathrm{Tr}\frac{\partial^2 v_d}{\partial k^2}\frac{nq_e^2}{6}}{en\left(v_d + \frac{1}{6}q_e^2 \mathrm{Tr}\frac{\partial^2 v_d}{\partial k^2}\right)}, \tag{2}$$

where $q = k - k_d$, $q_e^2 = \Sigma_q q^2 f_q / \Sigma_q f_q$, $v_d = (1/\hbar)(\partial\varepsilon/\partial k)|_{k=k_d}$, and $1/m_d = (1/\hbar^2)(\partial^2\varepsilon/\partial k^2)|_{k=k_d}$. The Taylor expansion becomes exact for the quadratic dispersion and the Peltier coefficient simplifies to

$$\Pi = \frac{1}{e}\left(-\mu + \varepsilon_d + \frac{5}{3}\frac{\hbar^2 q_e^2}{2m}\right). \tag{3}$$

In nondegenerate limit, the third term in the Peltier coefficient becomes

$$\frac{\hbar^2 q_e^2}{2m} = \frac{3\mathrm{PL}(5/2, -e^{\beta_e\mu})}{\beta_e \mathrm{PL}(3/2, -e^{\beta_e\mu})} \approx \frac{3}{2}k_B T_e, \tag{4}$$

where PL is the polylog function defined as $\mathrm{PL}(n,z) = \Sigma_{k=1}^{\infty} z^k/k^n$. To relate the electronic temperature to the relaxation time, we use the energy conservation,

$$\int_T^{T_e} c_v dT = \tau_E \sigma F^2 \approx \frac{3n}{2}k_B(T_e - T). \tag{5}$$

Here c_v is the heat capacity per unit volume, T_e is the electronic temperature, τ_E is the energy relaxation time [Eq. (5) can be taken as the definition of τ_E], σ is the electrical conductivity, and F is the electric field. After substituting Eqs. (4) and (5) into Eq. (3), we find that the Peltier coefficient is

$$\Pi = \frac{\varepsilon_d + 5/2k_B T_e - \mu}{e}, \tag{6}$$

$$\Pi = -\frac{\mu}{e} + \frac{5k_B T}{2e} + \frac{m}{2e^3 n^2}\left(1 + \frac{10\tau_E}{3\tau_{\mathrm{av}}}\right)J^2, \tag{7}$$

where τ_{av} is defined as $\tau_{\mathrm{av}} = \langle E\tau(E)\rangle / \langle E\rangle$; $\tau(E)$ is the characteristic time which describes how the distribution function relaxes.[11]

In degenerate limit, we have

$$\frac{\hbar^2 q_e^2}{2m} = \frac{3\mathrm{PL}(5/2, -e^{\beta_e\mu})}{\beta_e \mathrm{PL}(3/2, -e^{\beta_e\mu})} \approx \frac{3}{5}\mu + \frac{3\pi^2}{10}\frac{(k_B T_e)^2}{\mu}. \tag{8}$$

Again T_e can be related to τ_E by

$$\int_T^{T_e} c_v dT = \tau_E \sigma F^2 \approx \frac{\pi^2}{6}k_B^2 g(\mu)(T_e^2 - T^2), \tag{9}$$

where $g(\mu)$ is the density of states per unit volume at the Fermi level. Finally for degenerate case the Peltier coefficient is

$$\Pi \sim \frac{\pi^2}{2}\frac{(k_B T)^2}{\mu e} + \frac{m}{2e^3 n^2}\left(1 + 4\frac{\tau_E}{\tau_{\mathrm{av}}}\right)J^2. \tag{10}$$

Decreasing total scattering rates result in stronger nonlinear transport, by which we mean the current is not linearly proportional to the electric field [Eq. (11) below]. However, it does not affect the nonlinearity of the Peltier coefficient as much, since the Peltier coefficient is the ratio of two nonlinear currents and the effect of increasing scattering rates cancels.

$$J_Q \sim \frac{\pi^2}{2}\frac{ne\tau(k_B T)^2}{\mu m}F + \frac{ne^3\tau_{\mathrm{av}}^3}{2m^2}\left(1 + 4\frac{\tau_E}{\tau_{\mathrm{av}}}\right)F^3. \tag{11}$$

In both degenerate and nondegenerate limits, nonlinear Peltier is proportional to the effective mass and it is inversely proportional to the square of the carrier concentration. We numerically checked the validity of these proportionalities for the intermediate doping concentrations and we found that these relations are valid even in the intermediate regime.

Figure 2 shows the results obtained from the Monte Carlo simulation for a parabolic band structure. In the nondegenerate limit, the curves are compared with analytical expression [Eq. (6)]. ε_d, T_e, and μ were extracted from the MC data. One might argue that the agreement we obtained in this figure is due to the assumption of a shifted Fermi-Dirac distribution in both cases. To show that this is a correct hypothesis, results obtained using the standard method of enforcing Pauli exclusion principle without any assumption on the electronic distribution [known as Lugli-Ferry method[12] LF] are also plotted. The agreement between the LF method and the other data suggests that the distribution function is a shifted Fermi-Dirac. In Fig. 2 we have also reported the re-

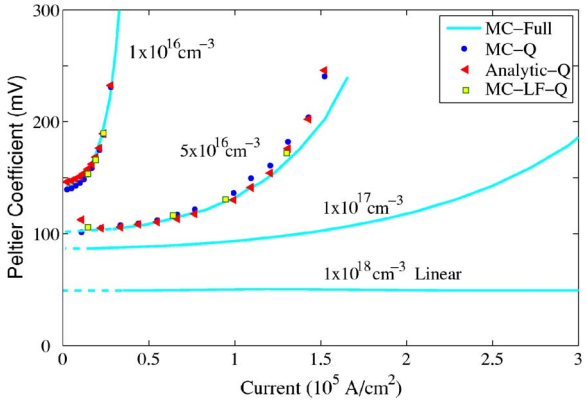

FIG. 2. (Color online) Q refers to quadratic band dispersion and Full refers to multivalley nonparabolic band structure. Results obtained from the Monte Carlo simulation by dividing the thermal current to the electrical current (circles) are shown in comparison with the analytical expression [Eq. (6)] using the Fermi level and electronic temperature obtained from the simulation (triangular). Results obtained using LF method are also shown to confirm the validity of the approach (squares). Solid lines are obtained from a more realistic band structure (nonparabolic). These are plotted for four different carrier concentrations. The above data are reported for n-type $In_{0.53}Ga_{0.47}As$ at room temperature. At high carrier concentrations Peltier coefficient tends to be linear.

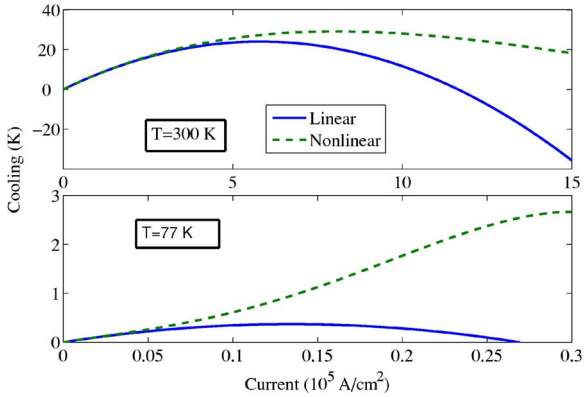

FIG. 3. (Color online) Linear and nonlinear theory predictions of the cooling efficiency of InGaAs at $T=300$ K and $T=77$ K. For each temperature the results are reported for the corresponding optimum dopings of the linear transport theory, which are 10^{18} and 5×10^{15} cm^{-3} for $T=300$ K and $T=77$ K, respectively.

sults from a more realistic band structure [multivalley nonparabolic uses $E(1+\alpha E)=\hbar^2k^2/2m$ with $\alpha_\Gamma=1.307$, $\alpha_L=0.691$, and $\alpha_x=0.202$ eV^{-1}].

When electronic temperature is higher than the lattice temperature, nonlinear behavior is observable. Nonlinearity is stronger for lower carrier concentrations. The reason is that at high concentrations, where the system is almost degenerate, the electron heat capacity is large and therefore much larger fields are required to heat up electrons. The e-ph coupling is another factor that determines the nonlinearity of the system. In materials with large e-ph coupling, electrons tend to thermalize faster with the lattice, therefore no heating takes place and transport stays linear. Figure 2 shows that for low carrier concentrations, nonlinear Peltier is relevant at currents on the order of 10^5 A cm^{-2} which is achievable in thin film thermoelectric elements.

At low temperatures the linear part of the Peltier coefficient decreases significantly. However, MC simulations show that the nonlinear part of the Peltier coefficient does not change as much. Therefore the nonlinear contribution becomes important in analyzing the efficiency of cryogenic solid state coolers and it can enhance their performance. The temperature difference created along a bulk sample due to an applied current can be obtained by

$$\Delta T = \frac{d}{k}\left(-\frac{1}{2}R_1 AJ^2 + \Pi_1 J\right) \quad \text{(linear)},$$

$$\Delta T = \frac{d}{k}\left[-\frac{1}{2}(R_1 + R_3 J^2)AJ^2 + (\Pi_1 + \Pi_3 J^2)J\right] \quad \text{(nonlinear)}, \tag{12}$$

where A is the area, k is the thermal conductivity, R is the resistance, Π_1 is the linear Peltier, and Π_3 is the third order Peltier coefficient (the total Peltier coefficient is $\Pi=\Pi_1+\Pi_3J^2$). Figure 3 shows the effect of including nonlinear contribution of the Peltier coefficient in the calculation of the cooling curve at room temperature and a low temperature of 77 K. According to the linear transport theory optimum doping at $T=300$ K is 10^{18} cm^{-3} and at $T=77$ K is 5×10^{15} cm^{-3}. Linear and nonlinear cooling curves [Eq. (12)] are plotted in Fig. 3 for these optimum doping concentrations. According to the figure, cooling efficiency is enhanced by 20% at room temperature and by 700% at $T=77$ K.

In summary, nonlinear Peltier coefficient is calculated analytically and numerically. Results show that nonlinearity occurs when electronic temperature starts to exceed the lattice temperature. Electronic heating is stronger when the electron heat capacity is low (that is the case for low doping concentrations) and when e-ph coupling is weak. Nonlinear Peltier coefficient is independent of the ambient temperature and it is proportional to the electronic mass and inversely proportional to the square of carrier concentration. The current threshold at which the Peltier coefficient becomes nonlinear depends on the carrier concentration. For InGaAs nonlinearity starts at 10^4 A/cm^2 for $n=10^{16}$ cm^{-3} and it increases to 10^5 A/cm^2 for $n=10^{17}$ cm^{-3}. These currents are achievable experimentally in thin film devices. The nonlinear Peltier effect can improve the cooling performance of thin film InGaAs microrefrigerators by 700% at 77 K.

This work was supported by ONR MURI Thermionic Energy Conversion Center.

[1] O. Kulik, J. Phys.: Condens. Matter **6**, 9737 (1994).
[2] A. N. Grigorenko, P. I. Nikitin, D. A. Jelski, and T. F. George, J. Appl. Phys. **69**, 3375 (1991).
[3] A. N. Grigorenko, P. I. Nikitin, D. A. Jelski, and T. F. George, Phys. Rev. B **42**, 7405 (1990).
[4] J. K. Freericks and V. Zlatic, Condens. Matter Phys. **9**, 603 (2006).
[5] E. N. Bogachek, A. G. Scherbakov, and U. Landman, Phys. Rev. B **60**, 11678 (1999).
[6] M. A. Çipiloğlu, S. Turgut, and M. Tomak, Phys. Status Solidi B **241**, 2575 (2004).
[7] A. S. Dzurak, C. G. Smith, L. Martin-Moreno, D. A. Ritchie, G. A. C. Jones, and D. G. Hasku, J. Phys.: Condens. Matter **5**, 8055 (1993).
[8] P. Reddy, S. Y. Jang, R. A. Segalman, and A. Majumdar, Science **315**, 1568 (2007). In the supplementary material, the measured thermovoltage as a function of temperature gradient is clearly nonlinear when a temperature difference of 20–30 °C is applied across single long-chain molecules.
[9] M. Zebarjadi, A. Shakouri, and K. Esfarjani, Phys. Rev. B **74**, 195331 (2006).
[10] M. Zebarjadi, C. Bulutay, K. Esfarjani, and A. Shakouri, Appl. Phys. Lett. **90**, 092111 (2007).
[11] M. Lundstrom, *Fundamentals of Carrier Transport*, 2nd ed. (Cambridge University Press, Cambridge, UK, 2000), Chap. 3, p. 132.
[12] P. Lugli and D. K. Ferry, IEEE Trans. Electron Devices **32**, 2431 (1985).